

Degenerate Fermi gas in a combined harmonic-lattice potential

P. B. Blakie¹, A. Bezett¹, P. F. Buonsante^{2,1}

¹Jack Dodd Centre for Photonics and Ultra-Cold Atoms, Department of Physics,
University of Otago, P.O. Box 56, Dunedin, New Zealand and

²Dipartimento di Fisica, Politecnico di Torino, Corso Duca degli Abruzzi 24, I-10129 Torino, Italy.

In this paper we derive an analytic approximation to the density of states for atoms in a combined optical lattice and harmonic trap potential as used in current experiments with quantum degenerate gases. We compare this analytic density of states to numerical solutions and demonstrate its validity regime. Our work explicitly considers the role of higher bands and when they are important in quantitative analysis of this system. Applying our density of states to a degenerate Fermi gas we consider how adiabatic loading from a harmonic trap into the combined harmonic-lattice potential affects the degeneracy temperature. Our results suggest that occupation of excited bands during loading should lead to more favourable conditions for realizing degenerate Fermi gases in optical lattices.

I. INTRODUCTION

Tremendous progress has been made in the preparation, control and manipulation of Fermi gases in the degenerate regime [1, 2, 3, 4, 5, 6, 7]. Such systems have many potential applications in the controlled study of fermionic superfluidity and the production of ultra-cold molecules. Another area of developing theoretical interest is in the physics of fermions in optical lattices [8, 9, 10, 11, 12], and experiments have already begun to examine the properties of Fermi-gases (prepared as boson-fermion mixtures) in one-dimensional [13, 14] and three-dimensional [15, 16, 17] optical lattices.

Optical lattices have many features in common with crystals where a periodic lattice is also present, and many of the ideas and techniques from solid state physics have been applied to this system. A unique property of optical lattices, as realized in experiments, is that the periodic lattice is accompanied by a harmonic confining potential, arising from an external magnetic trap or from effects related to the focused laser beams used to form the lattice. We shall refer to this potential as the *combined harmonic-lattice potential*, which is the main subject of the investigation presented in this paper (see Fig. 1).

Whilst the harmonic potential and *translationally invariant* periodic potential are well characterized individually, their properties when combined are not as well-understood. Even though the harmonic trap is often much weaker than the confinement provided by each lattice site, its effect on the spectrum and properties of the system can hardly be considered small: it breaks the translational invariance of the system and changes the nature of the energy states in the deep lattice from compressed bands, to a set of unbounded overlapping bands. Several recent articles have considered aspects of this system [12, 18, 19, 20]. In the context of a tightbinding model of ultra-cold bosons, the spectrum of the combined potential appears to have been first considered by Polkovnikov *et al.* [21]. Refs. [18, 19] have made detailed studies of the combined potential spectrum (also within a tightbinding description), and closed-form solutions to this problem were recently given by Rey *et al.* [20]. In Refs. [12, 22] an ideal gas of fermions in a 1D combined potential was examined without making the tightbinding approximation. All of these studies have con-

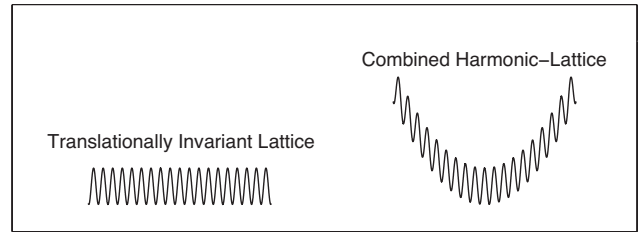


Figure 1: Schematic diagram comparing the translationally invariant lattice to the combined harmonic lattice considered in this paper.

firmed that, for appropriate parameter regimes, parts of the single particle spectrum will contain localized states. This is in contrast to the translationally invariant system, where interatomic interactions or disorder are needed for localization to occur (e.g. see [23, 24]). In the combined potential localization arises solely from single-particle effects. Experiments with ultra-cold (though non-condensed) bosons [25] have provided evidence for these localized states.

Many of the physical phenomena that are suitable to experimental investigation in optical lattices are sensitive to temperature and it is therefore of great interest to understand how the temperature of a quantum degenerate gas changes with lattice depth. Experimental results by Kastberg *et al.* [26] in 1995 showed that loading laser cooled atoms into a three-dimensional optical lattice caused the atoms to increase their temperature [35]. In previous work we have studied how the depth of a translationally invariant lattice affects the thermodynamic properties of quantum degenerate Bose [27] and Fermi [28] systems. The most important predictions of those studies relate to the temperature changes induced by the lattice, in particular that in appropriate regimes increasing the lattice depth could be used to cool the system. For Fermi gases this cooling effect was used to predict that loading into an optical lattice could be used to enhance the conditions for observing the superfluid transition [8]. However, recent work with a tightbinding model has shown that including the effects of the harmonic potential leads to an increase in the temperature of the system (compared to the Fermi temperature) by a factor of 2 [29], demonstrating the importance of fully treating

the combined potential.

In this paper we consider the thermal properties of a Fermi gas in the combined harmonic-lattice potential including the role of higher vibrational states. We derive an analytic approximation to the single-particle density of states and compare this analytic density of states to numerical solutions and determine validity criteria. We give characteristic energy and atom-number scales which can be used to predict when higher band effects will be important. Applying these density of states to a degenerate Fermi gas we consider how adiabatic loading from a harmonic trap into the combined harmonic-lattice potential affects the degeneracy temperature over a wide parameter regime. Our results show that beyond tightbinding effects provide an appreciable correction to the adiabatic loading calculations presented in Ref. [29]. Also, in the regime where higher band states are appreciably occupied, we find that the degeneracy temperature tends to increase to a lesser extent or even reduce during loading, suggesting that this regime might be useful for preparing a strongly degenerate Fermi gas in an optical lattice.

II. FORMALISM

A. Analytic density of states in the inhomogeneous lattice potential

Here we consider the properties of a system described by the single particle Hamiltonian

$$H = -\frac{\hbar^2}{2m} \nabla^2 + V_c, \quad (1)$$

where the *combined* potential V_c is formed by an optical lattice potential and harmonic trap potential, i.e.

$$V_c = V_h + V_l, \quad (2)$$

$$V_h = \frac{1}{2}m(\omega_x^2 x^2 + \omega_y^2 y^2 + \omega_z^2 z^2), \quad (3)$$

$$V_l = V_0[\sin^2(kx) + \sin^2(ky) + \sin^2(kz)]. \quad (4)$$

The harmonic trap is taken to be anisotropic, with angular frequencies $\{\omega_x, \omega_y, \omega_z\}$ along the coordinate directions. The lattice is of depth V_0 , k is the wavevector of the counter-propagating light fields used to form the lattice and $a = \pi/k$ is the direct lattice vector. We also use k to define the recoil frequency $\omega_R = \hbar k^2/2m$, and associated recoil energy $E_R = \hbar\omega_R$. The combined harmonic-lattice potential, as defined in Eqs. (2)-(4) has minima (i.e. lattice sites) at positions $\mathbf{r} = n_x a\hat{\mathbf{x}} + n_y a\hat{\mathbf{y}} + n_z a\hat{\mathbf{z}}$, where $\{\hat{\mathbf{x}}, \hat{\mathbf{y}}, \hat{\mathbf{z}}\}$ are unit vectors, and $\{n_x, n_y, n_z\}$ are integers that are convenient for labelling particular lattice sites. We note that our highly symmetric choice of the lattice potential, having a site coincident with the minimum of the harmonic potential, may be rather difficult to arrange experimentally. However, our primary interest is in the thermodynamic properties of the system which are insensitive to this symmetry.

We are interested in the limit where the lattice dominates the short-length scale properties of the system, and will take

$a \ll a_{ho}$, where $a_{ho} = \min\{\sqrt{\hbar/m\omega_j}\}_{j=x,y,z}$ is the smallest harmonic oscillator length. This removes our need to consider systems where extremely tight harmonic confinement causes all the atoms to coalesce to a single site.

1. 1D spectrum

Viverit *et al.* [12] have shown for the one-dimensional case of Eq. (1) that when the lattice is sufficiently deep the eigenstates are localized to lattice sites. For our symmetric potential the eigenstate localized at site n will necessarily also localize at site $-n$, so strictly we should not call such states localized. However, this property is fragile to any asymmetry in the system, and has no discernible effect on the energy spectrum (which is of primary interest to us). In this regime, the lattice site index n forms a convenient quantum number for the eigenstates, specifying the site where the state is localized. The respective energy eigenvalue is given by the value of the harmonic potential at that site, i.e.

$$\epsilon_n^{(0)} = \frac{1}{2}ma^2\omega^2n^2, \quad (5)$$

where ω is the trap frequency and we have set to zero the zero-point energy associated with the confinement in each lattice site. We will refer to these states as *ground band* states for clarity. The condition for localization is $\Delta E(n) > J_0$, where $\Delta E(n) \equiv \epsilon_{n+1}^{(0)} - \epsilon_n^{(0)}$ is the difference in (harmonic trap) potential energy between lattice site n and $n+1$, and J_0 is the tunneling between sites [36]. This requirement is most difficult to satisfy near the trap potential minimum, where the difference in energy between adjacent sites is least. This validity condition is equivalent to

$$|n| > n_{\text{crit}} \equiv q/8, \quad (6)$$

where n_{crit} is the approximately the index of the closest site to the origin for which the localization condition is satisfied and $q \equiv 8J_0/m\omega^2a^2$ is a dimensionless parameter which we discuss below (originally defined in [20]).

While states satisfying Eq. (5) are valid for sufficiently large values of n , this expression neglects the existence of excited vibrational states, which for the case of a translationally invariant lattice would correspond to the first excited band. The energy scale for the emergence of these excitations is ϵ_{gap} , and an analytic approximation for this quantity is calculated in Appendix A. Like the ground band states, these states will also localize when the difference between potential energy at neighbouring sites exceeds the tunneling matrix element for the first excited band, which we denote J_1 . Where this condition is satisfied the spectrum of these states will take the analytic form

$$\epsilon_n^{(1)} = \frac{1}{2}ma^2\omega^2n^2 + \epsilon_{\text{gap}}. \quad (7)$$

For clarity we shall refer to these as the *first excited band* states. This argument could be extended to additional bands of states, in particular, at an energy of roughly $2\epsilon_{\text{gap}}$ the next

vibrational states will be accessible. However, the tunneling rate J_m increases with the band index m , making the localization condition more difficult to satisfy, and analytic estimates for the energy gap to higher bands less accurate. Indeed, for single particle energies large compared to the lattice depth the spectrum will cross over to that of a harmonic oscillator. Additionally, for typical experimental parameters, the first two bands include sufficiently many states, and a large enough energy range to provide an accurate description of the system. Of course, high temperatures, or large lattice constants would require consideration of additional bands.

2. 3D spectrum and density of states

For more than one spatial dimension the wavefunction localization may be broken by neighbouring sites which have approximately the same local potential value. However since Eq. (1) is separable, the 3D ground band spectrum is completely determined by the one dimensional results (5) and (7), and under the assumption of localized states (see below), the ground and first excited band spectra are given by the expressions

$$\epsilon_{n_x n_y n_z}^{(0)} = \frac{1}{2} m a^2 (\omega_x^2 n_x^2 + \omega_y^2 n_y^2 + \omega_z^2 n_z^2), \quad (8)$$

$$\epsilon_{n_x n_y n_z}^{(1)} = \frac{1}{2} m a^2 (\omega_x^2 n_x^2 + \omega_y^2 n_y^2 + \omega_z^2 n_z^2) + \epsilon_{gap}, \quad (9)$$

respectively. Because of the lattice symmetry, there are 3 equivalent (and completely overlapping) first excited bands. Thus each energy state specified by the quantum numbers $\{n_x, n_y, n_z\}$ in (9) is three-fold degenerate [37]. This degeneracy would be broken if the lattice depth was different in each direction causing the first excited bands to separate in energy, but we do not consider that case here. The separability of the potential means that the validity conditions discussed for the one-dimensional case apply immediately, using the respective trap frequency in each direction, i.e. $n_j > n_{\text{crit}}^{(j)}$ $j = x, y, z$, where $n_{\text{crit}}^{(j)}$ is n_{crit} evaluated according to (6) using the trap frequency along direction- j .

The density of states for the spectra in Eqs. (8) and (9) is given by

$$g_c(\epsilon) = \frac{16}{\pi^2} \left(\frac{\omega_R}{\bar{\omega}} \right)^{3/2} \frac{\epsilon^{1/2}}{(\hbar \bar{\omega})^{3/2}} \quad (10)$$

$$+ \frac{48}{\pi^2} \left(\frac{\omega_R}{\bar{\omega}} \right)^{3/2} \frac{(\epsilon - \epsilon_{gap})^{1/2}}{(\hbar \bar{\omega})^{3/2}} \theta(\epsilon - \epsilon_{gap}),$$

where $\theta(x)$ is the unit step function, and $\bar{\omega} \equiv \sqrt[3]{\omega_x \omega_y \omega_z}$. The first term, corresponding to the ground band contribution to the density of states, exhibits a $\sqrt{\epsilon}$ -scaling with energy, similar to that of a homogeneous gas of free particles [29]. The second term includes the contribution of the first excited band states that occur at energies $\epsilon > \epsilon_{gap}$. As was noted in our discussion of the validity conditions of the spectra, additional bands will become accessible at $\epsilon \sim 2\epsilon_{gap}$, and so Eq. (10) should only be used in situations where $k_B T$ and the Fermi energy are much less than $2\epsilon_{gap}$.

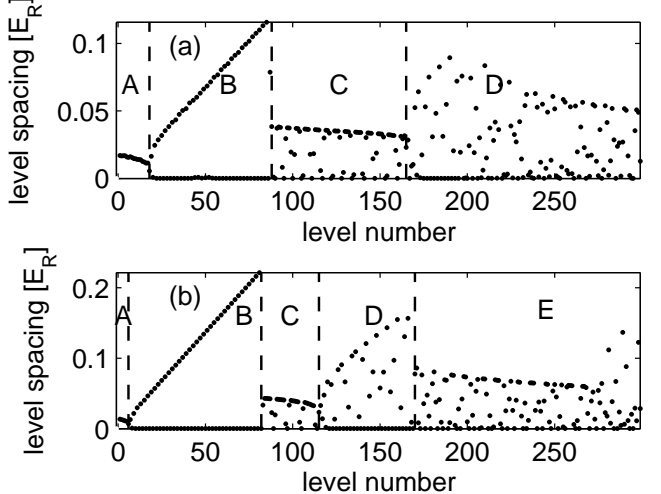


Figure 2: Energy level spacing for the 1D eigenspectrum relevant to the experimental setup in Ref. [16]. (a) $V_0 = 5E_R$, $\omega = 0.024\omega_R$ (b) $V_0 = 10E_R$, $\omega = 0.033\omega_R$. Parameters derived for ^{40}K with lattice made from counter propagating $\lambda = 826\text{nm}$ lasers with harmonic confinement arising from the focused lasers (beam waist taken to be $50\mu\text{m}$). Labels A-E explained in text.

B. Numerical Results for single particle spectrum

1. 1D spectrum

Here we show some typical results of the 1D spectrum of the combined potential in Fig. 2. In Refs. [18, 19, 20, 21] a detailed analysis of the spectrum has also been made, but in the tight binding (Hubbard) limit where only the vibrational ground state of each lattice site are included. Those studies considered a wide parameter regime of trapping frequencies and lattice depths, however in the tight-binding limit a single parameter describing the ratio of tunneling to harmonic potential is sufficient to characterize the nature of the eigen-spectrum. Several choices of parameter are used in the literature, and we follow the choice of Rey *et al.* [20] who define $q \equiv 4J_0/(\frac{1}{2}m\omega^2 a^2)$. With the inclusion of higher bands this single parameter by itself is insufficient to characterize the spectrum and both the lattice depth and harmonic confinement parameters are independently important. In Fig. 2 we show the level spacing obtained from numerical diagonalization of the one-dimensional case of Eq. (1). The parameters for this calculation were taken to correspond to those of the experiment [16]. For Fig. 2(a) with $V_0 = 5E_R$ we find that $q \approx 193$ and for Fig. 2(b) with $V_0 = 10E_R$ we find that $q \approx 28$. It is useful to compare our results to Fig. 1(b) of Ref. [19] to assess the effects of higher band states on the spectrum. We have segmented our spectrum with vertical dashed lines and indicated the characteristic regions by the letters A-E, which we explain: In region A tunneling dominates over the offset between lattice sites and the eigenstates are delocalized (for these states Eq. (5) will be a poor approximation). In region B localized states emerge which are approximately degener-

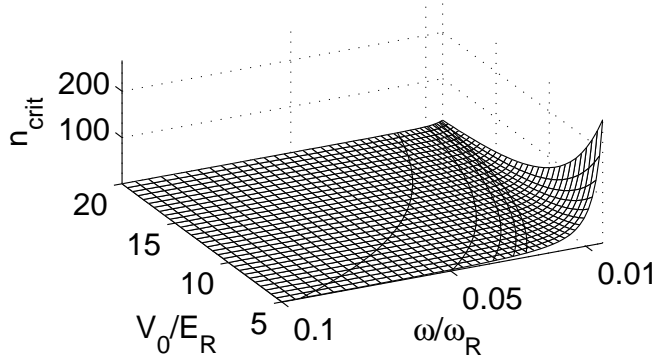


Figure 3: The critical site number for localization, as defined in Eq. (6), as a function of lattice depth and harmonic trap frequency. Contour lines are shown for $n_{\text{crit}} = 1, 3, 5$ and 7.

ate in energy (the spacing between every second eigenvalue is approximately zero). Because of the localizations (and applicability of Eq. (5)), the energy spacing between degenerate pairs increases linearly throughout this region. Regions A and B, as identified in Fig. 2, are equivalent to those in Fig. 1(b) of Ref. [19], and in general we find that the tightbinding description is in good qualitative agreement with our more general analysis. For the next regions (i.e. C, D etc.) the role of higher bands is essential and cannot be described within a simple tightbinding model. Region C has a similar appearance to region A, and consists of delocalized excited band states. The scatter in level spacing seen in C occurs because ground band states are also available in this energy range. In region D the excited bands state have become localized (similar to what happened in region B to the ground band states). In region E we have reached a sufficiently high energy scale that a 3rd band of states have begun to contribute.

The harmonic confinement used in Fig. 2 originates from the dipole confinement provided by the focused lasers used to make the lattice[38], and as the lattice depth increases so does the strength of harmonic confinement. We note that for Fig. 1(b) of [19] $q \approx 13 \times 10^6$ which is many orders of magnitude away from that found in current experiments [39]. The number of states in region A roughly scales as \sqrt{q} [20] so that in experimentally realized lattices region A is quite small and the majority of ground band states are well-localized.

2. Critical site index

In Fig. 3 we present n_{crit} (6) for a wide range of lattice depths and trap frequencies (note that we have used band structure calculations in a translationally invariant lattice to determine J_0 for each value of V_0). We observe that n_{crit} is large for small trap frequencies and shallow lattices so that only neighboring lattice sites quite far from the harmonic trap minimum have a sufficiently large potential difference to tunneling ratio to cause eigenstate localization. In such cases the analytic approximation for the eigenspectra given in Eqs. (8) and (9), and density of states given in Eq. (10) will not be

valid, and the result of the full numerical diagonalization will be necessary.

With increasing lattice depth the ground band tunneling matrix element decreases and the potential difference to tunneling ratio increases. Thus we find that n_{crit} decreases with increasing V_0 . Similarly, increasing the harmonic trap frequency also leads to a decrease in n_{crit} . The particular value of n_{crit} that justifies the use of our analytic density of states (10) depends on the parameters of system under consideration. If the system extends over N_s lattice sites in each direction, then $n_{\text{crit}} \ll N_s$ will be sufficient to ensure that the majority of the occupied states are well described by the localized spectrum.

3. Density of states

Equation (10) for the density of states in the combined potential is one of the central results of this paper. In this section we present numerical results to confirm the validity regime of this expression. To do this we diagonalize Eq. (1) to obtain the single particle eigen-spectrum $\{\epsilon_j\}$ for various trap frequencies and lattice depths. For the purposes of comparison to the analytic results, it is useful to construct a smoothed density of states, defined as

$$\bar{g}(\epsilon) = \frac{1}{2\Delta\epsilon} \int_{\epsilon-\Delta\epsilon}^{\epsilon+\Delta\epsilon} \sum_j \delta(\epsilon - \epsilon_j), \quad (11)$$

giving the average number of eigenstates with energy lying within $\Delta\epsilon$ of ϵ .

In Fig. 4 we compare the numerically calculated smoothed density of states against the analytic result $g_c(\epsilon)$ for various lattice depths in an isotropic trap of frequency $\bar{\omega} = 0.051\omega_R$. Agreement between the analytic and numerical calculations is seen to improve as the lattice depth increases. We also observe that at energies greater than approximately twice the gap energy the analytic and numerical results begin to differ more significantly as the contribution of additional bands become important (the gap energy in each case is the energy at which the cusp in the analytic density of states occurs).

It is of interest to more closely examine the reliability of the analytic density of states at low energy scales and for weak harmonic traps. In Fig. 5 we show such a comparison for an isotropic trap of frequency $\bar{\omega} = 0.01\omega_R$. For $V_0 = 4E_R$ the analytic result is in poor agreement with the numerical result, as the low energy states in this case are not localized. For $V_0 = 8E_R$ and more so $V_0 = 12E_R$, the analytic result is seen to provide a useful description of the numerical density of states. To quantify the degree of agreement seen in these results it is useful to consider the energy of the (first) localized state at site $n \approx n_{\text{crit}}$, i.e. $\epsilon_{\text{crit}} = m\bar{\omega}^2 a^2 n_{\text{crit}}^2 / 2$, indicated as vertical dashed lines in Fig. 5. The quantity ϵ_{crit} is the energy scale above which the ground band states become localized, and hence the lowest energy at which spectrum (5) is valid. For the case of $V_0 = 4E_R$, ϵ_{crit} exceeds ϵ_{gap} so that no states in the ground band are localized below the energy scale at which excited band states become accessible. For the case

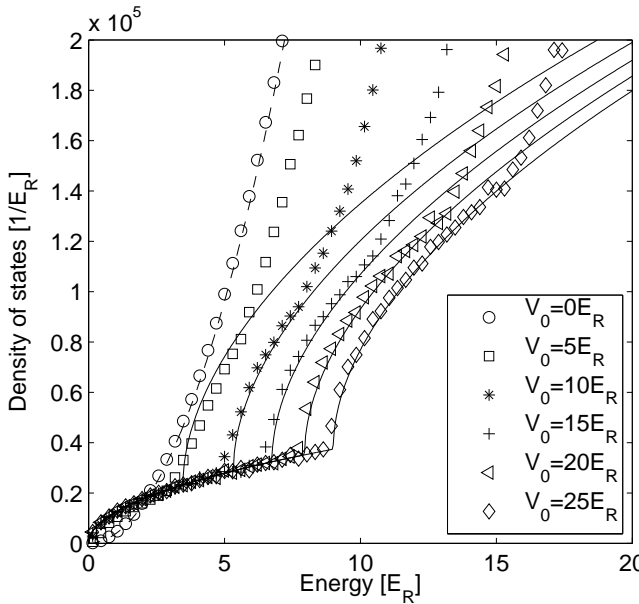


Figure 4: Density of states for $\bar{\omega} = 0.051\omega_R$. Numerical results for the density of states are shown using various markers (as labeled in the figure). The analytic density of states given in Eq. (10) is plotted for the cases with $V \geq 5E_R$ (solid line), using the expression $\epsilon_{gap} = 2\sqrt{V_0 E_R} - E_R$ for the band gap energy. The harmonic oscillator density of states is also shown (dashed line). The averaging interval used for the smoothed density of states is $\Delta\epsilon = 0.303E_R$.

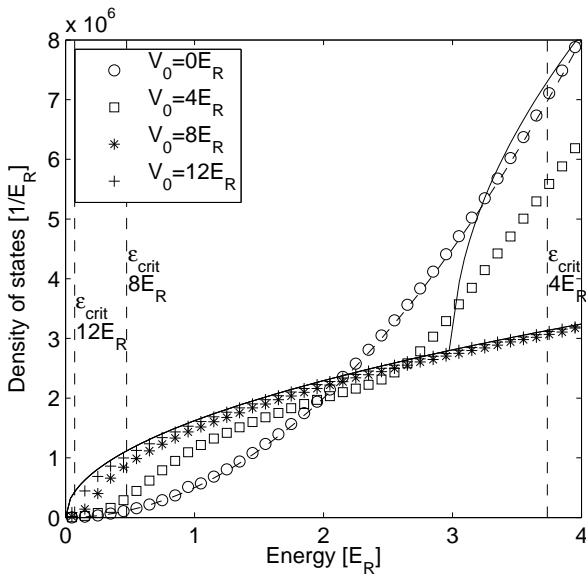


Figure 5: The density of states for a combined harmonic trap and lattice in the loose trap limit. Isotropic harmonic trap with trap frequency $\bar{\omega} = 0.01\omega_R$. The critical energy, given by $\epsilon_{crit} = m\bar{\omega}^2 a^2 n_{crit}^2 / 2$, is shown as a dashed vertical line and labeled by its corresponding lattice depth. The averaging interval used for the smoothed density of states is $\Delta\epsilon = 0.10E_R$.

of $V_0 = 8E_R$, $\epsilon_{crit} \simeq 0.5E_R$ and for energies above this better agreement between the analytic and numerical results

is observed in Fig. 5. For $V_0 = 12E_R$ the critical energy is $\epsilon_{crit} \simeq 0.07E_R$ and the analytic density of states furnishes better agreement at much lower energies.

In summary, we make the following observations about our analytic expression for the density of states:

1. Within its regime of validity, the analytic density of states provides an accurate description at intermediate energy scales, i.e. at energies above ϵ_{crit} where the spectrum is well-localized, yet below $\epsilon \sim 2\epsilon_{gap}$ where additional bands become accessible.
2. The agreement between the analytic density of states and numerical calculations improves with increasing lattice depth and increasing trap frequency.

III. APPLICATIONS TO FERMI GASES

A. General Properties

1. Fermi energy

The Fermi energy in the combined harmonic-lattice potential, $\epsilon_{F,c}$, is determined from the number of particles in the system according to

$$N = \int_0^{\epsilon_{F,c}} d\epsilon g_c(\epsilon). \quad (12)$$

To compute the Fermi energy from our analytic result (10) it is convenient to define the *cusp number* [40] N_c as the number of particles for which $\epsilon_{F,c} = \epsilon_{gap}$. Because the energy gap depends on the lattice depth, so does N_c . Using Eqs. (10) and (12) we obtain

$$N_c = \frac{32}{3\pi^2} \left(\frac{\omega_R}{\bar{\omega}} \right)^{3/2} \left(\frac{\epsilon_{gap}}{\hbar\bar{\omega}} \right)^{3/2}. \quad (13)$$

For $N < N_c$ (i.e. $\epsilon < \epsilon_{gap}$) only the first term in the density of states (10) is nonzero in Eq. (12) and we can invert to obtain the Fermi energy

$$\epsilon_{F,c} = \left(\frac{3\pi^2 N}{32} \right)^{2/3} \frac{\hbar\bar{\omega}^2}{\omega_R}, \quad N < N_c. \quad (14)$$

For $N > N_c$ excited band states contribute. In this case a general analytic expression for the Fermi energy in terms of N is not available, but for $(N - N_c) \ll N_c$ we make a series expansion of the integral of the density of states about ϵ_{gap} . This expression can then be solved perturbatively to yield the approximate expression

$$\epsilon_{F,c} = \epsilon_{gap} \left\{ 1 + \delta - \frac{2\delta^{3/2}}{1 + 3\delta^{1/2}} \right\}, \quad 0 < \delta \ll 1 \quad (15)$$

where $\delta \equiv 2(N - N_c)/3N_c$ is the small parameter.

It is also convenient to define the *cusp depth* V_c , as the lattice depth at which $\epsilon_{F,c} = \epsilon_{gap}$. The cusp depth is a function

of the number of particles and harmonic trap frequency, given by

$$V_c = \frac{\hbar\omega_R}{4} \left[\left(\frac{3\pi^2 N}{32} \right)^{2/3} \left(\frac{\bar{\omega}}{\omega_R} \right)^2 + 1 \right]^2, \quad (16)$$

where we have made use of the analytic expression relating ϵ_{gap} to V_0 , as derived in Appendix A.

The two cusp parameters characterize the interesting features of the combined harmonic-lattice system and can be interpreted as follows:

- N_c : For a system with fixed combined potential (i.e. fixed V_0 , $\{\omega_j\}$), N_c is the maximum number of atoms that can be accommodated in the ground band only. For $N > N_c$ the $T = 0$ ground state of the system will contain excited band states.
- V_c : For a system with fixed atom number and harmonic trap frequencies, V_c is the smallest lattice depth for which the atoms can be accommodated in the ground band. For $V_0 < V_c$ the $T = 0$ ground state of the system will contain excited band states.

These parameters motivate us to emphasize the distinctive properties of the energy spectrum in the combined potential as compared to the usual periodic lattice case. In the translationally invariant lattice, there is a fixed number of single particle states in each band (equal to the number of lattice sites), and for sufficiently deep lattices (typically $V_0 \gtrsim 2E_R$) the ground and first excited bands occupy disjoint energy regions separated by a finite energy gap. In contrast, for the combined harmonic-lattice potential, the energy bands are overlapping and can only be differentiated by the local nodal structure of the wavefunctions at each site, where they have a spatial character approximately given by harmonic oscillator states (see Appendix A). This local structure of the wavefunctions is apparent in experiment, and leads to states of different bands (as we have defined them here) residing in distinctive regions of momentum space in expansion images (e.g. see Refs. [16, 30]). If it is desirable to restrict the system to access only states of the ground band, so as to realize a system well-described by a Hubbard model, then according to our above prescription this necessarily requires $N < N_c$ or equivalently $V_0 > V_c$, in addition to having sufficiently low temperature.

B. Sommerfeld analysis of isentropic loading of a degenerate Fermi gas

The properties of a quantum degenerate Fermi gas can be approximated by the Sommerfeld expansion (e.g. see [31]). Of particular interest is the expression for entropy $S = \frac{\pi^2}{3} g(\epsilon_F) k_B^2 T$, valid for $T \ll T_F$, where $g(\epsilon_F)$ is the

density of states evaluated at the Fermi energy, ϵ_F . For many applications to Fermi gas experiments, the parameter of most interest is the degeneracy parameter $t \equiv k_B T / \epsilon_F$, i.e. the ratio of the temperature to the Fermi temperature, for which the Sommerfeld expression can be written as

$$S = \frac{\pi^2}{3} \epsilon_F g(\epsilon_F) k_B t. \quad (17)$$

Here we consider the change in degeneracy temperature of a Fermi gas as it is slowly loaded from a harmonic trap into the combined harmonic-lattice potential, as is done in experiments. To characterize this temperature change we assume that the loading is *isentropic* so that the initial entropy in the harmonic potential (with initial degeneracy temperature t_i) is the same as the final entropy when the system is in the combined harmonic-lattice potential (with final degeneracy temperature t_f). Within the validity regime of the Sommerfeld relation (17), the ratio of these temperatures is given by

$$\frac{t_f}{t_i} = \frac{\kappa_h(N)}{\kappa_c(N)}, \quad (t_i, t_f \ll 1) \quad (18)$$

obtained by assuming that S remains constant, where we have introduced the dimensionless extensive parameter $\kappa_x(N) \equiv \epsilon_{F,x} g_x(\epsilon_{F,x})$ ($x = h, c$), with $g_h(\epsilon)$ and $\epsilon_{F,h}$ the density of states and Fermi energy for a harmonic trap respectively. We have chosen to express κ as a function of N rather than ϵ_F , since the number of atoms remains constant during the loading procedure, whereas the Fermi energy may change significantly.

For the purely harmonic trap $g_h(\epsilon) = \epsilon^2 / (2\hbar^3 \bar{\omega}^3)$ and $\epsilon_{F,h} = \hbar\bar{\omega}(6N)^{1/3}$ (e.g. see [32]), which give

$$\kappa_h(N) = 3N. \quad (19)$$

For $N < N_c$, the excited band states do not contribute to κ_c and using results (10) and (14) we obtain

$$\kappa_c(N) = \frac{3}{2}N, \quad N < N_c. \quad (20)$$

Thus for $N < N_c$ the ratio of degeneracy temperatures will increase by a factor of two. Because N_c is a monotonically increasing function of V_0 , it might be expected that for sufficiently deep final lattice depth we will always obtain this factor of 2 increase in the degeneracy temperature. However, N_c decreases with increasing $\bar{\omega}$, and since $\bar{\omega}$ may change with lattice depth (e.g. if the lattice is produced by focused lasers) a large final lattice depth may in fact lead to $N > N_c$. We also note that when $N < N_c$ the ratio of the degeneracy temperatures (18) is independent of the harmonic trap frequency, even if this parameter changes during the loading [41]. Similar conclusions to those presented in this section are given in Ref. [29].

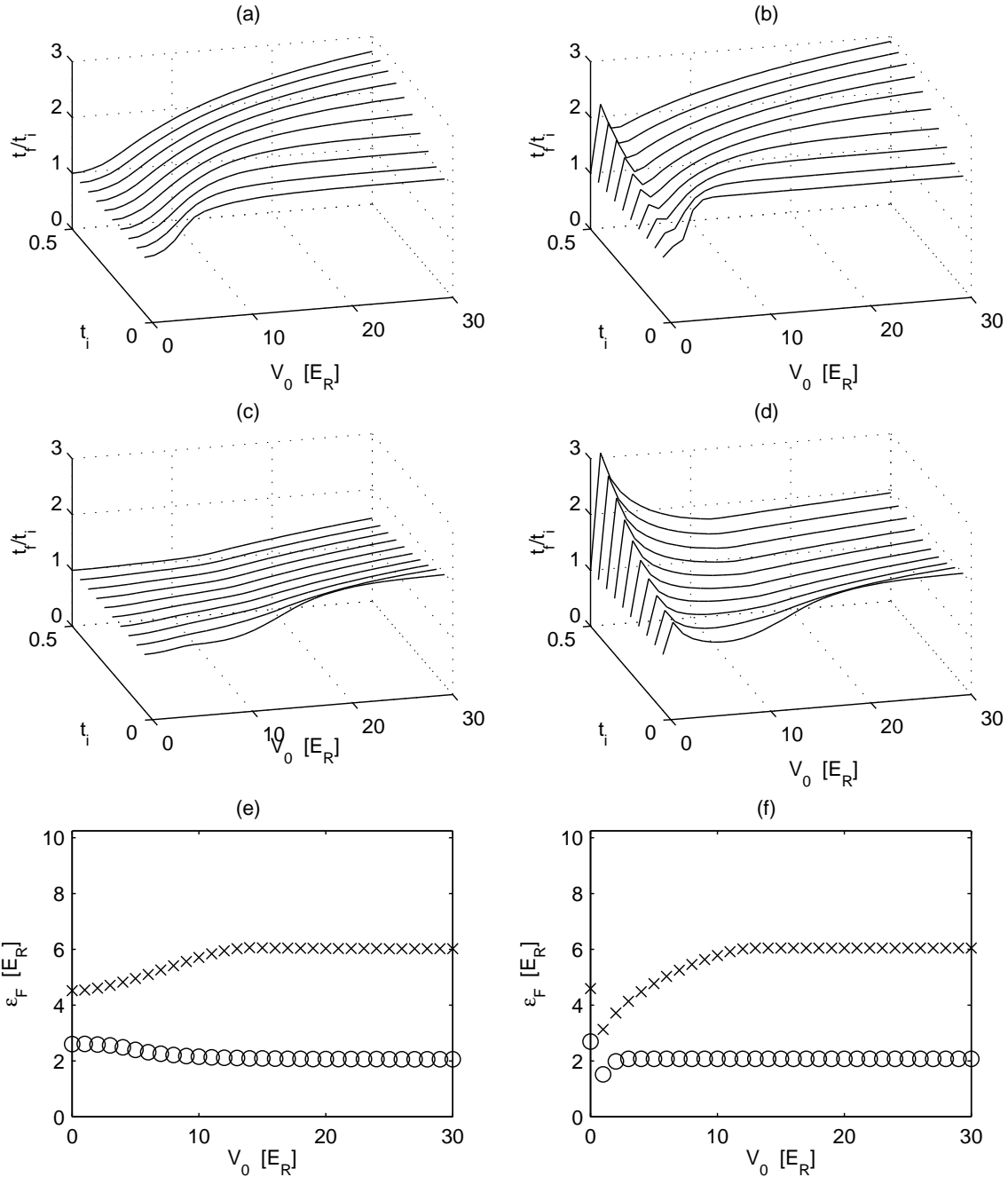


Figure 6: Temperature of an ideal Fermi gas isentropically loaded into a combined harmonic-lattice potential. The ratio of the final degeneracy temperature (after loading) to the initial degeneracy temperature in the harmonic trap are shown for various initial temperatures and lattice depths for the case (a) $N = 50 \times 10^3$ and (c) $N = 250 \times 10^3$. In (e) the Fermi energy is shown as a function of lattice depth for $N = 25 \times 10^3$ (circles), $N = 250 \times 10^3$ (crosses). (b), (d) and (f) correspond to (a), (c) and (e) respectively, but are calculated using the analytic density of states (10). For all results we have used an isotropic harmonic trap of frequency of $\bar{\omega} = 0.04\omega_R$.

C. Numerical results for isentropic loading of the combined harmonic-lattice

In this section we numerically examine the temperature of an ideal Fermi gas loaded into a combined harmonic-lattice

potential for a range of lattice depths. Our main results are calculated using the energy spectrum found by numerically diag-

onalizing (1). To determine the temperature under this type of loading we calculate the entropy of a gas of N fermions over a range of temperatures and lattice depths, i.e. $S(T, V_0, \vec{\omega}, N)$, where $\vec{\omega} = \{\omega_x, \omega_y, \omega_z\}$. We numerically invert this function to find temperature as a function of the other quantities $T(S, V_0, \vec{\omega}, N)$, and by examining the behaviour of T for fixed S , we can predict the temperature of the gas as a function of lattice depth.

Our procedure for determining entropy is as follows: The single particle spectrum $\{\epsilon_j\}$ of the lattice is calculated for given values of $\vec{\omega}$ and V_0 . We then calculate the partition function \mathcal{Z}

$$\log \mathcal{Z} = \sum_j \log \left(1 + e^{-\beta(\epsilon_j - \mu)} \right), \quad (21)$$

where μ is found by ensuring particle conservation. The entropy of the system can then be expressed as

$$S = k_B (\log \mathcal{Z} + \beta E - \mu \beta N), \quad (22)$$

where $\beta = 1/k_B T$, and $E = -\partial \ln \mathcal{Z} / \partial \beta$ is the mean energy.

In Figs. 6(a)-(f) we show the properties of an isentropically loaded gas for various parameters. In Figs. 6(a) and (c) we show the ratio of the final to initial reduced temperatures for $N = 50 \times 10^3$ and $N = 250 \times 10^3$ respectively. In both cases, the reduced temperature is seen to increase as the lattice depth increases. For $N = 50 \times 10^3$ atoms the critical lattice depth is $V_c \approx 2.3E_R$. For the lowest initial reduced temperature (i.e. the front-most curve in 6(a)) we see that the reduced temperature increases by a factor of two by the time that V_0 increases beyond V_c , in agreement with the predictions of Eqs. (18)-(20) (also see Ref. [29]). Similarly, for the case of $N = 250 \times 10^3$ atoms, $V_c \approx 12.4E_R$ and for the lowest temperature result in Fig. 6(c), we see that the reduced temperature increases by a factor of two as V_0 increases beyond this value of V_c . For higher initial temperatures the Sommerfeld result does not hold. In Figs. 6(a) and (c) we see that the warmer systems (larger t_i values) have the contrasting behaviour of heating up more or less than the Sommerfeld prediction respectively. In that regime the degeneracy temperature is dominated by the change in the Fermi energy that occurs during the lattice loading procedure, as shown in Fig. 6(e). That is, for the case in Fig. 6(a) [6(c)] the Fermi energy tends to decrease [increase] with increasing lattice depth.

In Fig. 6(c) (and to a lesser extent in 6(a)) we see that while excited bands are occupied (i.e. for $V < V_c$) the degeneracy temperature increases by a factor of less than 2. This suggests that having excited bands occupied might provide more favourable conditions for investigating fermionic superfluidity in lattices. Additionally, because the tunneling rate is larger for higher bands it may be more easy to reversibly manipulate the lattice in this regime.

In Figs. 6(b), (d), (f) we show the results equivalent to those in Figs. 6(a), (c), (e), but calculated using the analytic density of states given in Eq. (10). Qualitatively the agreement between the results is good for $V_0 \gtrsim 4E_R$. The main discrepancy is observed for small V_0 values where the role of non-localized states and higher bands is important.

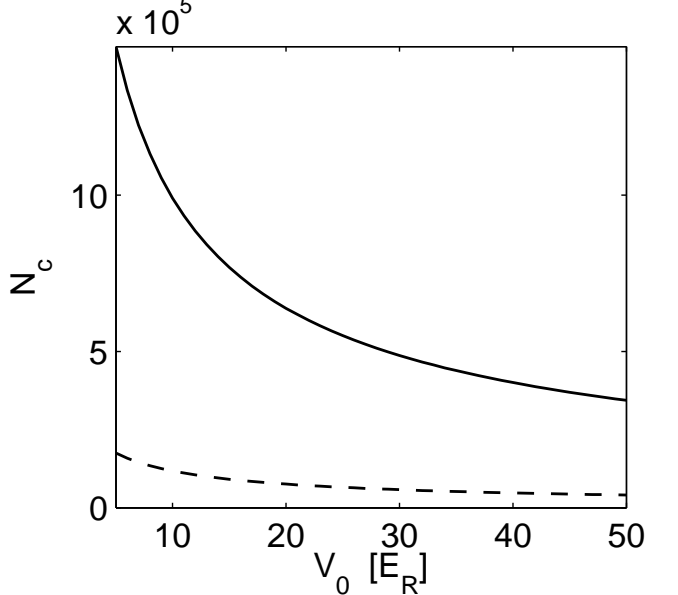


Figure 7: N_c for the case of ^{40}K in a lattice formed by focused lasers (solid) $\lambda = 826\text{nm}$ with $70\mu\text{m}$ waist, (dashed) $\lambda = 1200\text{nm}$ with $50\mu\text{m}$ waist.

IV. RELATION TO EXPERIMENTS

It is of interest to compare how important excited band effects might be for current experiments. In Fig. 7 we show N_c for parameters similar to those used in recent experiments by the ETH group [15, 16]. In those experiments up to 10^5 atoms were prepared in each spin state. Because the harmonic confinement increases with lattice depth ($\bar{\omega} \sim \sqrt{V_0 E_R} / \hbar$), we find that the Fermi energy will eventually lie in the first excited band, but only for very large lattice depths ($V_0 \gtrsim 280E_R$). We also consider a longer wavelength lattice made from lasers with $\lambda = 1200\text{nm}$ with slightly tighter focus (beam waist of $50\mu\text{m}$) for which the recoil energy and the gap to higher bands is smaller. In such a configuration (dashed curve) we see that higher bands would become important for much lower atom numbers.

In Fig. 8 we consider the effect of loading on the degeneracy temperature for parameters relevant to the experiment in Ref. [15]. The results in Fig. 8(a) are for the same parameters considered by Köhl who made a calculation in the tightbinding limit (see Fig. 1 of Ref. [29]). We broadly find agreement with those results, however make note of several differences. First, at the lowest depths considered ($V_0 \sim 5E_R$) Köhl observed the reduced temperature to initially decrease with increasing lattice depth. In contrast our results, which are valid for all lattice depths, do not exhibit this feature, and instead are seen to smoothly connect with the $V_0 = 0E_R$ (purely harmonic case). We conclude that in this region the tightbinding approximation and the neglect of higher bands is not valid.

Second, in Köhl's results the reduced temperature is observed to saturate to a value of twice that of the initial harmonic trap when the lattice is sufficiently deep (typically

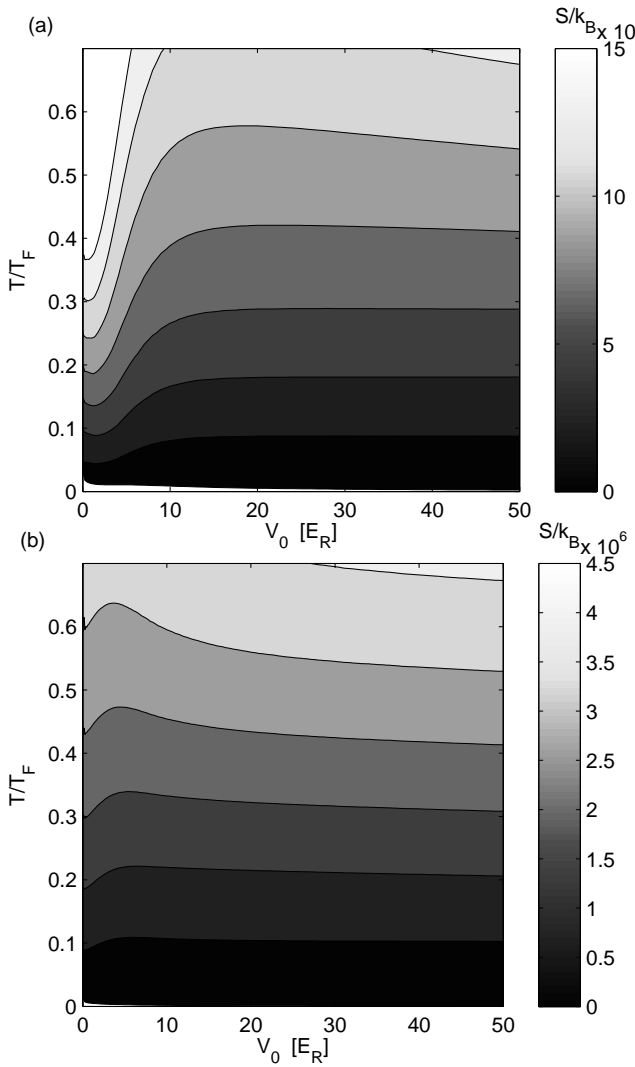


Figure 8: Degeneracy temperature for isentropic loading of ^{40}K into an optical lattice. (a) $N = 50,000$ and (b) $N = 750,000$. Parameters correspond to solid line in 7. Additional harmonic confinement of frequency $\omega = 0.005\omega_R$ is superimposed on the confinement due to the focused beam waist to make the spectrum well-behaved as $V_0 \rightarrow 0$.

$V_0 \gtrsim 15E_R$). Many of our high temperature curves instead show a slight decrease in reduced temperature as the depth of the lattice increases. We have verified that this behaviour is due to higher band states, and that if we neglect them from our calculations our results saturate in agreement with those in [29]. This indicates that even when the deep lattice behaviour is dominated by the ground band (i.e. we have $N < N_c$), if a small number of atoms are able to thermally access excited band states they can have a significant effect on the temperature of the system during loading.

In Fig. 8(b) the same parameters are used, except the number of atoms is increased to 750,000. According to Fig. 7 for this number of atoms $V_c \approx 15E_R$. In this case we see that only a small increase in the degeneracy temperature oc-

urs during loading and ultimately for sufficiently large final lattice depth (i.e. $V_0 \gtrsim 20E_R$) the reduced temperature is observed to be approximately the same as in the initial harmonic trap. We note that this result requires the occupation of higher bands and cannot be analysed using a tightbinding approach.

The discussion in this section shows that while current experiments are likely not strongly affected by higher bands, the parameter regime where they become important is rather close. Experiments could enter this regime by using larger wavelength lattices or tighter harmonic confinement (e.g. more tightly focused lasers to produce the optical lattice).

V. CONCLUSIONS

We have discussed the nature of the spectrum of a Fermi gas in a combined harmonic trap and optical lattice potential. Using this spectrum we have derived an analytic density of states that is relatively accurate for the lattice depths and harmonic confinements used in experiments. We have characterized the validity criteria for this density of states and have used it to characterise a Fermi gas in the combined potential. As an application we have examined how adiabatic loading from a harmonic trap into the combined harmonic-lattice potential affects the degeneracy temperature of an ideal Fermi gas. Our results show that when excited band states are occupied the system is less heated by the lattice loading, and may be less sensitive to non-adiabatic effects, suggesting that this regime is worthy of further investigation in experiments.

Acknowledgments

PBB would like to acknowledge useful discussions with M. Köhl and support from the Marsden Fund of New Zealand. P.B. acknowledges a grant from the *Lagrange Project*–CRT Foundation and is grateful to the Jack Dodd Centre for the warm hospitality

Appendix A: ANALYTIC APPROXIMATION TO BAND GAP ENERGY

In this section we derive an analytic expression for the band gap in deep lattices. We go beyond the usual harmonic oscillator approximation and obtain results equivalent to those used in Ref. [33].

We will consider the standard harmonic approximation the optical lattice potential, by making a Taylor expansion about the lattice site minimum at $x = 0$, i.e.

$$V = \frac{V_0}{2}[1 - \cos(bx)] \approx \frac{V_0 b^2}{4}x^2 - \frac{V_0 b^4}{48}x^4. \quad (\text{A1})$$

Casting the harmonic term in the form of a harmonic oscillator potential, $\frac{1}{2}m\omega_{\text{Latt}}^2x^2$, yields the effective harmonic oscillator frequency of $\omega_{\text{Latt}} = \sqrt{V_0 b^2/2m}$, and the localized states in the optical lattice can be approximated as harmonic

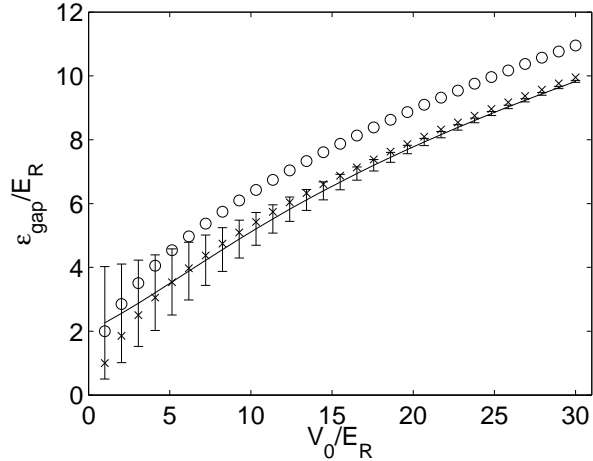


Figure 9: Comparison between numerically determined energy gap for a 1D sinusoidal lattice (solid), with the upper and lower limits corresponding to the band gap at the center and the edge of the Brillouin Zone. The harmonic approximation, $\hbar\omega_{\text{Latt}} = 2\sqrt{V_0 E_R}$ (circles) and the estimate treating the quartic expansion perturbatively, $\epsilon_{\text{gap}} = 2\sqrt{V_0 E_R} - E_R$ (crosses).

oscillator states. This approximation neglects the influence of tunneling between sites that gives a quasimomentum dependence, and predicts that the band gap is equal to $\hbar\omega_{\text{Latt}}$. For our purposes it is desirable to go beyond this approximation and obtain a more accurate analytic expression for the band gap energy. To do this we use the harmonic oscillator states

to treat the quartic term in Eq. (A1) perturbatively. This is most easily done using the normal ladder operators, so that $x^4 = \left(\frac{\hbar}{2m\omega_{\text{Latt}}}\right)^2 (a^\dagger + a)^4$, which gives the 1st order shifts in the oscillator state energies as

$$\Delta E_n = -\frac{E_R}{4}(2n^2 + 2n + 1). \quad (\text{A2})$$

Thus the approximate energies of the localized states are given by

$$E_n = \left[2\sqrt{\frac{V_0}{E_R}}(n + 1/2) - \frac{1}{4}(2n^2 + 2n + 1) \right] E_R. \quad (\text{A3})$$

Of most interest is the difference in energy between the $n = 0$ and $n = 1$ states, which provides an estimate of the energy gap between the ground and first excited bands, i.e.

$$\epsilon_{\text{gap}} = 2\sqrt{V_0 E_R} - E_R. \quad (\text{A4})$$

We see that treating the quartic term leads to a 1 recoil suppression of the band gap compared to the harmonic oscillator frequency. In Fig. 9 we compare this analytical expression with the band gap determined numerically by evaluating the full band structure of the $\frac{V_0}{2}[1 - \cos(bx)]$ potential. For shallow lattices the band gap is strongly dependent on the value of quasimomenta considered and error bars indicate the range of energy gaps from band centre to band edge.

[1] B. DeMarco and D. S. Jin, *Science* **285**, 1703 (1999).
[2] F. Schreck, L. Khaykovich, K. L. Corwin, G. Ferrari, T. Bourdel, J. Cubizolles, and C. Salomon, *Phys. Rev. Lett.* **87**, 080403 (2001).
[3] K. M. O'Hara, S. L. Hemmer, M. E. Gehm, S. R. Granade, and J. E. Thomas, *Science* **298**, 2179 (2002).
[4] G. Modugno, G. Roati, F. Riboli, F. Ferlaino, R. J. Brecha, and M. Inguscio, *Science* **297**, 2240 (2002).
[5] S. Gupta, Z. Hadzibabic, M. W. Zwierlein, C. A. Stan, K. Dieckmann, C. H. Schunck, E. G. M. van Kempen, B. J. Verhaar, and W. Ketterle, *Science* **300**, 1723 (2003).
[6] C. A. Regal, C. Ticknor, J. L. Bohn, and D. S. Jin, *Nature* **424**, 47 (2003).
[7] J. Cubizolles, T. Bourdel, S. J. J. M. F. Kokkelmans, G. Shlyapnikov, and C. Salomon, *Phys. Rev. Lett.* **91**, 240401 (2003).
[8] W. Hofstetter, J. I. Cirac, P. Zoller, E. Demler, and M. D. Lukin, *Phys. Rev. Lett.* **89**, 220407 (2002).
[9] P. Rabl, A. J. Daley, P. O. Fedichev, J. I. Cirac, and P. Zoller, *Phys. Rev. Lett.* **91**, 110403 (2003).
[10] L. Santos, M. A. Baranov, J. I. Cirac, H.-U. Everts, H. Fehrmann, and M. Lewenstein, *Phys. Rev. Lett.* **93**, 030601 (2004).
[11] M. Rigol and A. Muramatsu, *Phys. Rev. A* **69**, 053612 (2004).
[12] L. Viverit, C. Menotti, T. Calarco, and A. Smerzi, *Phys. Rev. Lett.* **93**, 110401 (2004).
[13] G. Modugno, F. Ferlaino, R. Heidemann, G. Roati, and M. Inguscio, *Phys. Rev. A* **68**, 011601(R) (2003).
[14] H. Ott, E. de Mirandes, F. Ferlaino, G. Roati, G. Modugno, and M. Inguscio, *Phys. Rev. Lett.* **92**, 160601 (2004).
[15] T. Stöferle, H. Moritz, K. Günter, M. Köhl, and T. Esslinger, *Phys. Rev. Lett.* **96**, 030401 (2006).
[16] M. Köhl, H. Moritz, T. Stöferle, K. Günter, and T. Esslinger, *Phys. Rev. Lett.* **94**, 080403 (2005).
[17] S. Ospelkaus, C. Ospelkaus, O. Wille, M. Succo, P. Ernst, K. Sengstock, and K. Bongs, *Phys. Rev. Lett.* **96**, 180403 (2006).
[18] C. Hooley and J. Quintanila, *Phys. Rev. Lett.* **93**, 080404 (2004).
[19] M. Rigol and A. Muramatsu, *Phys. Rev. A* **70**, 043627 (2004).
[20] A. M. Rey, G. Pupillo, C. W. Clark, and C. J. Williams, *Phys. Rev. A* **72**, 033616 (2005).
[21] A. Polkovnikov, S. Sachdev, and S. M. Girvin, *Phys. Rev. A* **66**, 053607 (2002).
[22] V. Ruuska and P. Törmä, *New J. Phys.* **6**, 59 (2004).
[23] D. Jaksch, C. Bruder, J. I. Cirac, C. Gardiner, and P. Zoller, *Phys. Rev. Lett.* **81**, 3108 (1998).
[24] P. Buonsante, V. Penna, A. Vezzani, and P. Blakie (2006), arXiv:cond-mat/0610476.
[25] H. Ott, E. de Mirandes, F. Ferlaino, G. Roati, V. Türck, G. Modugno, and M. Inguscio, *Phys. Rev. Lett.* **92**, 120407 (2004).
[26] A. Kastberg, W. D. Phillips, S. L. Rolston, R. J. C. Spreeuw, and P. S. Jessen, *Phys. Rev. Lett.* **74**, 1542 (1995).
[27] P. B. Blakie and J. V. Porto, *Phys. Rev. A* **69**, 013603 (2004).
[28] P. B. Blakie and A. Bezzett, *Phys. Rev. A* **71**, 033616 (2005).

- [29] M. Köhl, Phys. Rev. A **73**, 031601(R) (2006).
- [30] J. H. Denschlag, J. E. Simsarian, H. Häffner, C. McKenzie, A. Browaeys, D. Cho, K. Helmerson, S. L. Rolston, and W. D. Phillips, J. Phys. B **35**, 3095 (2002).
- [31] K. Huang, *Statistical Mechanics* (Wiley, 1967).
- [32] D. Butts and D. Rokhsar, Phys. Rev. A **55**, 4346 (1997).
- [33] I. Spielman, P. R. Johnson, J. Huckans, C. Fertig, S. Rolston, W. Phillips, and J. Porto, Phys. Rev. A **73**, 020702 (2006).
- [34] P. B. Blakie and C. W. Clark, J. Phys. B **37**, 1391 (2004).
- [35] In fact this study used adiabatic de-loading to reduce the temperature of the constituent atoms.
- [36] We determine J_0 using band structure calculations, see [34]
- [37] This is in addition to the degeneracy arising from spatially equivalent lattice sites, e.g. for $\{n_x, n_y, n_z\}$ all non-zero there are 8 states of the same energy found by taking $\{\pm n_x, \pm n_y, \pm n_z\}$.
- [38] The harmonic frequency is given by $\omega = \sqrt{8V_0/mw^2}$ where w is the beam waist (also see [29]).
- [39] We calculate that $q = 13 \times 10^6$ roughly corresponds to a $V_0 = 4E_R$ deep lattice and harmonic confinement of oscillator frequency 0.8 Hz.
- [40] So named, because the corresponding Fermi energy sits at the cusp in the analytic density of states (e.g.. see Fig. 4).
- [41] However, the absolute temperature does depend on the trap frequency.